SHED-Derived Exosomes Regulate Microglial Polarization in the Treatment of Traumatic Brain Injury in Rats via miR-330-5p

Ye Li
Xi'an Jiaotong University
Xinxin Wang
Xi'an Jiaotong University
Xiaoyu Cao
Xi'an Jiaotong University
Na Li
Xi'an Jiaotong University
Sun Meng
Xi'an Jiaotong University
Ang Li (drliang@mail.xjtu.edu.cn)
College of Stomatology, Xi'an Jiaotong University

Research

Keywords: Traumatic brain injury, Exosomes, miR-330-5p, Microglia

Posted Date: August 28th, 2020

DOI: https://doi.org/10.21203/rs.3.rs-65521/v1

Abstract

Background: Traumatic brain injury (TBI) causes structural damage and impairs motor and cognitive function of the brain. Our previous study suggested that exosomes (EXs) secreted by stem cells from human exfoliated deciduous teeth (SHED) extenuated motor damage in TBI rats by regulating microglia. The molecular mechanism of SHED-EXs was investigated in the present study.

Methods: The miRNA array was performed to determine the differential miRNA expression in SHED-EXs treating microglia. The key miRNA was selected. Flow cytometry, immunofluorescence, enzyme linked immunosorbent assay (ELISA) and Griess assay were performed to detect the function of key miRNA. Real-time PCR, Western blotting and dual luciferase reporter assay were used to confirm the relationship between key miRNA and the target gene. Chromatin immunoprecipitation (ChIP) was performed to determine the downstream pathway of EXs-miRNA. Traumatic brain injury rat model was established and local injection of EXs-miRNA was performed to evaluate the effect.

Results: SHED-EXs delivery of miR-330-5p was the key in the regulation of microglia polarization by inhibiting M1 polarization and promoting M2 polarization. Mechanistically, miR-330-5p had an inhibitory effect on Ehmt2, and miR-330-5p/Ehmt2 promoted the transcription of CXCL14 through H3K9me2. In vivo data showed that SHED-EXs/miR-330-5p reduced neuro-inflammation and repaired neurological function of TBI rats.

Conclusions: SHED-EXs/miR-330-5p improved the motor function of rats after TBI by inhibiting M1 polarization and promoting M2 polarization of microglia through Ehmt2/H3K9me2/CXCL14 pathway.

Introduction

Traumatic brain injury (TBI) refers to local anatomical and pathological structural damage in the brain due to trauma, which can cause hemiplegia, aphasia, mental retardation, or even coma and death [1–3]. Currently, surgery and drugs are commonly used as symptomatic treatments. However, these approaches can only control intracranial pressure and maintain blood pressure in patients, whereas their overall efficacies in altering prognoses are poor [4]. A large volume of experimental studies have shown that transplantation of stem cells from multiple sources can improve the function of damaged neurons in animal models of TBI [5–10]. More importantly, stem cells from human exfoliated deciduous teeth (SHED) represent a promising cell type to restore the function of damaged neurons since they express neuronal surface markers, have the ability to differentiate into neurons, and promote neuronal proliferation [11–13]. However, the therapeutic effect and potential mechanism remains to be clarified.

In recent years, more and more studies have shown that paracrine signaling is a key mechanism by which stem cell transplantation carries out its effects. Furthermore, exosomes (EXs) are important components during this process [14]. After secretion by donor cells, they are internalized by recipient cells and biological molecules within are released, thereby improving the biological functions of recipient cells [15, 16]. EXs are mixed vesicles that consist of different components. In addition to characteristic proteins

and lipids in cellular membranes, it is noteworthy that these vesicles carry a class of nucleic acids, namely microRNAs (miRNAs), that can inhibit target genes in recipient cells to regulate their functions [17, 18].

Our previous study showed that SHED can signal to microglia via secretion of EXs to regulate the polarization and repair neuronal damage resulting from TBI in rats [19]. Therefore, in the present study, we employed microarrays, real-time PCR, immunofluorescence, flow cytometry, chromatin immunoprecipitation, and animal experiments to determine the key substances by which SHED exosomes (SHED-EXs) carry out their effects in ameliorating TBI, as well as to explore their downstream effector mechanisms. Collectively, our findings may provide theoretical and experimental bases for the application of SHED and their secreted exosomes in TBI treatment and other future clinical applications.

Materials And Methods

SHED-EXs isolation

Immortalized TERT-SHED were used in the present study as in our previous report [19]. Dulbecco's modified Eagle's medium (DMEM) containing 1% penicillin/streptomycin (all from Gibco, USA) was used to culture TERT-SHED for 48 hours. Culture medium was collected for EXs isolation. ExoQuick-TC Exosome Precipitation Solution (EXOTC50A-1-SBI, BioCat, Germany) was used according to the instructions of the manufacturer.

miRNA microarray

1 μg/ml LPS stimulated BV-2 cells (obtained from Chinese Academy of Sciences) were co-cultured with 100 μg/ml SHED-EXs for 48 hours. LPS stimulated BV-2 and co-cultured BV-2 were obtained for RNA extraction. RNA samples were sent for miRNA microarray analysis (Genechem, Shanghai, China). Fold change of more than 2-fold (up- or downregulated) ($p < 0.001$) were chosen.

Real-Time PCR

Real-Time PCR were performed to validate array data. 1 μg/ml LPS stimulated BV-2 cells were co-cultured with 100 μg/ml SHED-EXs for 48 hours. LPS stimulated BV-2 and co-cultured BV-2 were obtained for RNA extraction. RNA was extracted with TRIzol regent (Code No. 15596026, Invitrogen, USA). Reverse transcription was performed with Mir-X miRNA First-Strand Synthesis Kit (Code No. 638315, Takara, Japan) according to the product manual. The reverse-transcribed cDNA was detected by Mir-X miRNA qRT-PCR TB Green® Kit (Code No. 638314, Takara, Japan).

miR-330-5p mimics and inhibitors transfection

miR-330-5p mimics and inhibitors were diluted to 50 nM. Lipofectamine 3000 were incubated with miR-330-5p mimics and inhibitors for 30 min at room temperature. Then, the transfection solution was used to culture BV-2 for 8 h. Transfection efficacy were evaluated by Real-Time PCR 48 h after transfection.

ELISA and Griess assay

ELISA kit (Code No. BMS603-2TWO, BMS607-3FIVE, BMS614INST, Thermo Fisher, USA) was used to detect the secretion of cytokines (IL-6, TNF-α and IL-10) of BV-2 according to the manufacturer's protocols. Griess assay were performed with the product manual of Griess Reagent Kit (Code No. G7921, Thermo Fisher, USA).

Flow cytometry

The expression of CD68 and CD206 were detected. Briefly, cells were collected and washed 3 times with PBS. Cell suspension was then blocked with bovine serum albumin (BSA) for 30 minutes. Incubated cells with Mouse Anti-Mouse CD68 (1:100, ab222914, Abcam, UK) and Rabbit Anti-Mouse CD206 (1:200, ab64693, Abcam, UK) for 1 h. Washed for 3 times.

Immunofluorescence

Cells were fixed with 4% PFA for 15 minutes and washed with PBS for 3 times. BSA was used to block for 30 minutes. Primary Rat Anti-CD68 antibody (1:200, ab53444, Abcam, UK) and Rabbit Anti-CD206 antibody (1:100, ab64693, Abcam, UK) were used for incubation overnight at 4 ° C. Secondary antibodies were used for incubation for 2 h. Nuclei were stained with DAPI.

Target prediction of miR-330-5p and luciferase reporter assay

Target predication for miR-330-5p was carried out using miRDB, microRNA.ORG and TargetScan. Intersection of the three database were obtained. Ehmt2 was chosen for its reported regulation of microglia development [20], so we speculated that it may also play an important role in the polarization of mature microglia. A recombinant plasmid containing Emmt2-Luc/Rluc was prepared. The binding site of miR-330-5p was completely mutated. Luciferase reporter assay was performed as previously described [21].

Western blotting

Western blotting was performed as previously described [21]. Primary antibodies used were Rabbit Anti-Ehmt2/G9a antibody (1:500, ab40542, Abcam, UK) and Mouse Anti-Histone H3 (di methyl K9) antibody (1:500, ab1220, Abcam, UK).

ChIP-qPCR

ChIP-qPCR was performed with ChIP Kit (Magnetic, qPCR) (ab270816, Abcam, UK) according to the manufacturer's protocols. Antibodies used were Rabbit Anti-EHMT2/G9A antibody and Mouse Anti-Histone H3 (di methyl K9) antibody.

SHED-EXs/ miR-330-5p Treatment for TBI Rats

Male wistar rats of about 200 g were used and were randomly assigned into five groups: Sham group (n = 6), TBI group (n = 6), TBI rats treated with DMEM (n = 6), TBI rats treated with SHED-EXs (n = 6) and TBI rats treated with miR-330-5p mimics (n = 6). TBI rat model was constructed as previously described [19]. Briefly, a circular window with a diameter of 2 mm was drilled at the cortical motor function area. A 20 gram weight was used to vertically hit the injured area from 15 cm high. For SHED-EXs group, 3 μl SHED-EXs (400 μg/ml) was injected locally into the injury site. For miR-330-5p mimics group, 3 μl miR-330-5p mimics (100 nM) was used. Brain tissues were collected 48 hours later for cytokines and immunostaining studies. The recovery of motor dysfunction was evaluated after 48 hours, 7 days, 14 days and 21 days.

Statistical Analysis

A p value of less than 0.05 was considered statistically significant. Student's t test and one-way ANOVA were performed between two groups and among multiple groups.

Results

Differentially expressed miRNAs in microglia after SHED-EXs treatment

Array data (Fig. 1A) showed that 27 miRNAs were upregulated and 39 miRNAs were downregulated after SHED-EXs was added to LPS-stimulated BV-2 cells, for which a two-fold change or more was used as the cutoff criterion for consideration of significantly altered miRNAs. We selected the most differentially expressed 10 miRNAs (6 up-regulated and 4 down-regulated miRNAs) and confirmed their expression by Real-time PCR (Fig. 1B, C). We found that changes in miR-330-5p expression were most significantly different. We further quantitated miR-330-5p expression after LPS stimulation of BV-2 cells and found that miR-330-5p expression was significantly downregulated (Fig. 1D). After addition of the EXs inhibitor, GW4869, no significant difference in miR-330-5p expression was shown compared with that of the LPS stimulation group (Fig. 1E). In summary, LPS stimulation significantly downregulated miR-330-5p in microglia. Furthermore, SHED-EXs delivery rescued miR-330-5p expression and may play a role as a key regulator in microglial function.

miR-330-5p inhibits microglial M1 polarization and promotes M2 polarization

In order to elucidate the specific function of miR-330-5p in microglia, miR-330-5p was first upregulated in BV-2 cells. Transfection efficiency was measured 48 h after transfection with miR-330-5p mimics (Fig. 2A). LPS stimulation of BV-2 cells increased the secretions of the pro-inflammatory factors IL-6 and TNF-α while miR-330-5p overexpression significantly reduced the secretions of these two cytokines. In addition, LPS stimulation decreased the secretion of the anti-inflammatory factor IL-10 while miR-330-5p overexpression significantly rescued the secretion (Fig. 2B). Furthermore, Griess assay was used to examine the effects of miR-330-5p overexpression on nitrite concentrations. LPS stimulation significantly increased nitrite concentrations while miR-330-5p overexpression significantly decreased these levels (Fig. 2C). Next, flow cytometry and immunofluorescence were used to determine changes in M1- and M2-polarization markers in BV-cells. Results showed that the expression of the M1 polarization marker CD68

was significantly increased while the expression of the M2 polarization marker CD206 was significantly decreased in BV-2 cells after LPS stimulation. In contrast, transfection with miR-330-5p mimics significantly downregulated CD68 expression and significantly upregulated CD206 expression (Fig. 2D–G). Real-time PCR results showed that the expression of the M1 polarization markers—CD11b, CD86, CD16, and MHCII—were significantly increased, while the expression levels of the M2 polarization markers, IL-10 and ARGINASE1, were significantly decreased after BV-2 cells were stimulated with LPS. miR-330-5p overexpression significantly inhibited M1 polarization marker expression and promoted M2 polarization marker expression (Fig. 2H, I). Collectively, miR-330-5p inhibited M1 polarization and promoted M2 polarization. **Appendix File 1** shows the effects of miR-330-5p inhibitors on BV-2 polarization.

miR-330-5p targets Ehmt2 to promote CXCL14 transcription through H3K9me2 in the regulation of microglial polarization

Next, we explored the downstream mechanism of miR-330-5p regulation. Three databases (Targetscan, microRNA.ORG, and miRDB) were used for target gene prediction of miR-330-5p and overlapping data from these three databases were obtained (Fig. 3A, **Appendix File 2**). From these data, we selected Ehmt2—which is associated with microglia development as a candidate target gene[20]. Real-time PCR was used to measure changes in Ehmt2 expression after miR-330-5p was upregulated. Results showed that miR-330-5p significantly inhibited Ehmt2 expression (Fig. 3B). Western blotting was used to validate the effects of miR-330-5p upregulation on Ehmt2 protein levels. Results showed that Ehmt2 expression was decreased when miR-330-5p was upregulated (Fig. 3C, D). A luciferase reporter plasmid containing either wild-type or mutant Ehmt2 was constructed (Fig. 3E) according to its predicted binding site and was co-transfected with either miR-330-5p mimics or miR-330-5p inhibitors into 293T cells. The luciferase reporter assay was used to determine the relationship between miR-330-5p and Ehmt2 (Fig. 3F).

Ehmt2 is a major methyltransferase that catalyzes mono-methylation and di-methylation of H3K9[22]. We found that miR-330-5p overexpression induced H3K9me2 downregulation (Fig. 3G). It was reported that H3K9me2 inhibits the transcription of CXCL14[20], a key factor in macrophage polarization[23]. Therefore, we further measured CXCL14 expression after transfection with miR-330-5p mimics. Real-time PCR results showed that miR-330-5p overexpression increased CXCL14 transcription (Fig. 3H). ChIP further showed that mir-330-5p inhibited the enrichment of Ehmt2 and H3K9me2 at the promoter region of CXCL14 (Fig. 3I, J).

Ehmt2 rescues the inhibition of M1 polarization and promotion of M2 polarization of microglia mediated by miR-330-5p

We stably overexpressed Ehmt2 in BV-cells, stimulated them with LPS, and transfected them with miR-330-5p mimics before measuring changes in the levels of the pro-inflammatory factors, IL-6 and TNF-α, and the anti-inflammatory factor, IL-10. Results showed that Ehmt2 reversed miR-330-5p-induced inhibition of pro-inflammatory factors, while exerting opposite effects on anti-inflammatory factors (Fig. 4A, B). Ehmt2 restored miR-330-5p-induced decreases in nitrite concentrations (Fig. 4C). Flow

cytometry, immunofluorescence, and Real-time PCR showed that Ehmt2 reversed miR-330-5p-induced inhibition of M1 polarization markers and miR-330-5p-induced promotion of M2 polarization markers in BV-2 cells (Fig. 4D–I).

miR-330-5p affects microglial polarization to ameliorate traumatic brain injury in rats

In order to determine whether SHED-EXs miR-330-5p has any *in vivo* effects, we established a rat model of TBI and used SHED-EXs and miR-330-5p for local-injection treatments at the wound site (Fig. 5A). Motor function tests were conducted in TBI rats at 48 h, one week, two weeks, and three weeks after injury. The BBB scoring showed significant motor dysfunction in all groups at 48 h after TBI, except for the sham group. Motor functions in the SHED-EXs group and miR-330-5p-mimics group were significantly improved after one week (Fig. 5B). Sectioning of brain tissues and hematoxylin and eosin (H&E) staining were carried out in the different groups of rats at two weeks after TBI. Results showed significant tissue defects in brain tissues from the TBI and DMEM groups, whereas significant recovery in brain tissue injuries were seen in the SHED-EXs group and miR-330-5p mimics group (Fig. 5C). Inflammation status was examined in the damaged brain tissues from different groups after 48 h of treatment. Results showed that the expression of the pro-inflammatory factors IL-6 and TNF-α were significantly lower in the SHED-EXs group and miR-330-5p mimics group compared with those in the TBI group and DMEM group, whereas the expression of the anti-inflammatory factor IL-10 was significantly increased (Fig. 5D, E).

Immunofluorescent staining was performed on brain tissue sections from the different groups. Results showed that the expression of the M1 polarization marker CD68 was significantly decreased in the SHED-EXs and miR-330-5p mimics groups, while the expression of the M2 polarization factor CD206 was significantly increased compared with those in the TBI group and DMEM group (Fig. 6).

Taken together, our present study found that miR-330-5p from SHED-EXs ameliorated functional impairment caused by TBI in rats. From a mechanistic perspective, TBI decreased miR-330-5p expression in microglia, and SHED-EXs delivery of miR-330-5p promoted M2 polarization and inhibited M1 polarization, thus reducing neuro-inflammation and promoting tissue repair through the downstream Ehmt2-H3K9me2-CXCL14 signaling axis (Fig. 7).

Discussion

Our *in-vitro* and *in-vivo* study demonstrated that SHED affected microglial polarization through miR-330-5p in exosomes to ameliorate neurological impairment caused by TBI in rats. In the present study, SHED was chosen to repair neurological damage. In addition to their potential clinical significance, our findings suggest that we may consider the perspective of an embryonic origin of stem cells in the treatment of disease. SHED and other odontogenic stem cells, such as dental pulp stem cells (DPSCs), all originate from neural crest cells during the embryonic stage [24, 25]. This may be the reason that the signals inside had better functionality. Therefore, odontogenic stem cells may be used as treatment substitutes for neural stem cells, the latter of which are ethically controversial to some extent. The application range of odontogenic stem cells was somehow expanded. From this perspective, future studies may focus on

other types of odontogenic stem cells to detect their neuro-restorative functions, which may provide more possible sources of stem cells in the treatment of TBI.

In order to clarify the potential mechanism of SHED-EXs in regulating microglial polarization, we performed a miRNA array to detect differentially expressed miRNAs. Several studies have shown that stem-cell-derived EXs perform their biological functions on target cells by delivering specific miRNAs. For example, the key to mesenchymal stem cell transplantation for myocardial infarction is in the miR-125b-5p contained within secreted EXs [26]. Bone marrow mesenchymal stem cells (BMSCs) exert their protective effects on ischemia-reperfusion via miR-199a-5p in their EXs [27]. BMSCs-derived EXs regulate age-related insulin resistance through the transfer of functional miR-29b-3p [28]. The present study showed that compared with BV-2 after LPS activation, the addition of SHED-EXs caused a significant upregulation of miR-330-5p expression in activated BV-2. We hypothesize that miR-330-5p was the key constituent in SHED-EXs that was effectively transferred to microglia. miR-330-5p expression was significantly down-regulated in BV-2 after LPS activation, suggesting that the effects of external stimuli on microglia may be mediated by miR-330-5p.

It has been reported that M2 polarization of microglia, which is beneficial for recovery, depends on the STAT6-mediated IL-4/IL-13 signaling pathway [29]. In a mouse autoimmune encephalomyelitis model, deletion of IL-4 inhibits M2 polarization and aggravates disease-related damage. In addition, the TGF-β1 pathway is active during M2 polarization [30]. Transcription factors such as NF-kB, C/EBP-β, and Notch/RBP-J also have important regulatory effects on the polarization of microglia [31–33]. In the present study, we demonstrated that Ehmt2 was responsible for the regulation of miR-330-5p in microglial polarization. Ehmt2 promoted M1 polarization, inhibited M2 polarization, and thus may also represent a potential target for TBI therapy.

Ehmt2 is a major histone methyltransferase that specifically catalyzes H3K9 dimethylation [34]. H3K9me2 has a binding site for heterochromatin protein 1 (HP1), which recruits transcriptional repressors to prevent gene activation [35]. In the adult central nervous system, chemokines and their receptors participate in developmental, physiological, and pathological processes, promote cellular interactions and activate and maintain central-nervous-system homeostasis [36]. CXCL14 is one of the oldest chemokines, but its function is not well known [37]. CXCL14 regulates hippocampal integrity and maintains balance in the adult brain. Therefore, the imbalance of CXCL14 can seriously affect the homeostasis of the nervous system. Our present study found that miR-330-5p inhibited the enrichment of Ehmt2 and H3K9me2 in the CXCL14 promoter region, thereby promoting the transcription of CXCL14, suggesting that the mechanism by which CXCL14 maintains nervous-system stability may be closely related to microglial polarization.

Cell-cell interactions are the primary mechanisms during stem cell therapy. Stem cells may directly secrete cytokines to remotely regulate the functions of recipient cells or indirectly carry out their functions through EXs [38, 39]. However, a continuous supply of effective factors is required for long-term treatment results [40]. In the present study, the effect of SHED-EXs/miR-330-5p was determined by a one-time injection, suggesting an efficacy “memory” mechanism of SHED-EXs/miR-330-5p transplantation.

Histone methylation-mediated epigenetic regulation may produce long-term effects as a stable regulatory factor.

Our present study demonstrated that SHED-EXs/miR-330-5p repaired motor function of rats with TBI. Hence, SHED-EXs/miR-330-5p is expected to represent a new strategy for treating TBI. Moreover, miR-330-5p and SHED-EXs could be combined to play their corresponding advantages in the system, thereby creating a new method for treating TBI. In addition, traditional drugs cannot cross the blood-brain barrier to function at the injury site. Due to the nanoscale size of SHED-EXs, future studies using intravenous injections of SHED-EXs are needed to determine their potential efficacies.

Conclusions

SHED-EXs delivery of miR-330-5p ameliorates functional impairment caused by TBI by promoting M2 polarization and inhibiting M1 polarization to reduce neuro-inflammation and promote tissue repair through the Ehmt2-H3K9me2-CXCL14 axis.

Abbreviations

ChIP: Chromatin immunoprecipitation

DMEM: Dulbecco's modified Eagle's medium

ELISA: enzyme linked immunosorbent assay

EXs: exosomes

SHED: stem cells from human exfoliated deciduous teeth

TBI: Traumatic brain injury

Declarations

ETHICS APPROVAL AND CONSENT TO PARTICIPATE

All animal experiments were reviewed and approved by the Ethics Committee of College of Stomatology, Xi'an Jiaotong University.

CONSENT FOR PUBLICATION

Not applicable

AVAILABILITY OF DATA AND MATERIAL

The data that support the findings of this study are available from the corresponding author upon reasonable request.

COMPETING INTERESTS

The authors declare no conflicts of interest to the authorship and/or publication of this article.

ACKNOWLEDGMENTS

Not applicable

FUNDING

This work is supported by the National Natural Science Foundation of China (No. 81701037).

AUTHOR's CONTRIBUTIONS

Y. L., contributed to conception, design, data acquisition, analysis, and interpretation, drafted and critically revised the manuscript; X. W., contributed to conception, design, data analysis and interpretation, critically revised the manuscript; X.C., N.L. and M. S., contributed to data acquisition, analysis, and interpretation, critically revised the manuscript; A. L., contributed to conception, design, data analysis and interpretation, drafted and critically revised the manuscript. All authors gave final approval and agreed to be accountable for all aspects of the present work.

References

1. Azouvi P, Arnould A, Dromer E, Vallat-Azouvi C. Neuropsychology of traumatic brain injury: An expert overview. Rev Neurol (Paris). 2017; 173: 461-72.
2. Dixon KJ. Pathophysiology of Traumatic Brain Injury. Phys Med Rehabil Clin N Am. 2017; 28: 215-25.
3. Najem D, Rennie K, Ribecco-Lutkiewicz M, Ly D, Haukenfrers J, Liu Q, et al. Traumatic brain injury: classification, models, and markers. Biochem Cell Biol. 2018; 96: 391-406.
4. Galgano M, Toshkezi G, Qiu X, Russell T, Chin L, Zhao LR. Traumatic Brain Injury: Current Treatment Strategies and Future Endeavors. Cell Transplant. 2017; 26: 1118-30.
5. Longhi L, Zanier ER, Royo N, Stocchetti N, McIntosh TK. Stem cell transplantation as a therapeutic strategy for traumatic brain injury. Transpl Immunol. 2005; 15: 143-8.
6. Riess P, Molcanyi M, Bentz K, Maegele M, Simanski C, Carlitscheck C, et al. Embryonic stem cell transplantation after experimental traumatic brain injury dramatically improves neurological outcome, but may cause tumors. J Neurotrauma. 2007; 24: 216-25.
7. Bakhtiary M, Marzban M, Mehdizadeh M, Joghataei MT, Khoei S, Pirhajati Mahabadi V, et al. Comparison of transplantation of bone marrow stromal cells (BMSC) and stem cell mobilization by granulocyte colony stimulating factor after traumatic brain injury in rat. Iran Biomed J. 2010; 14: 142-9.

8. Lee DH, Lee JY, Oh BM, Phi JH, Kim SK, Bang MS, et al. Functional recovery after injury of motor cortex in rats: effects of rehabilitation and stem cell transplantation in a traumatic brain injury model of cortical resection. Childs Nerv Syst. 2013; 29: 403-11.
9. Wang S, Cheng H, Dai G, Wang X, Hua R, Liu X, et al. Umbilical cord mesenchymal stem cell transplantation significantly improves neurological function in patients with sequelae of traumatic brain injury. Brain Res. 2013; 1532: 76-84.
10. Thomaidou D. Neural stem cell transplantation in an animal model of traumatic brain injury. Methods Mol Biol. 2014; 1210: 9-21.
11. Miura M, Gronthos S, Zhao M, Lu B, Fisher LW, Robey PG, et al. SHED: stem cells from human exfoliated deciduous teeth. Proc Natl Acad Sci U S A. 2003; 100: 5807-12.
12. Aghajani F, Hooshmand T, Khanmohammadi M, Khanjani S, Edalatkhah H, Zarnani AH, et al. Comparative Immunophenotypic Characteristics, Proliferative Features, and Osteogenic Differentiation of Stem Cells Isolated from Human Permanent and Deciduous Teeth with Bone Marrow. Mol Biotechnol. 2016; 58: 415-27.
13. Gonmanee T, Thonabulsombat C, Vongsavan K, Sritanaudomchai H. Differentiation of stem cells from human deciduous and permanent teeth into spiral ganglion neuron-like cells. Arch Oral Biol. 2018; 88: 34-41.
14. Spees JL, Lee RH, Gregory CA. Mechanisms of mesenchymal stem/stromal cell function. Stem Cell Res Ther. 2016; 7: 125.
15. Phinney DG, Pittenger MF. Concise Review: MSC-Derived Exosomes for Cell-Free Therapy. Stem Cells. 2017; 35: 851-8.
16. Riazifar M, Pone EJ, Lotvall J, Zhao W. Stem Cell Extracellular Vesicles: Extended Messages of Regeneration. Annu Rev Pharmacol Toxicol. 2017; 57: 125-54.
17. Dreyer F, Baur A. Biogenesis and Functions of Exosomes and Extracellular Vesicles. Methods Mol Biol. 2016; 1448: 201-16.
18. van Niel G, D'Angelo G, Raposo G. Shedding light on the cell biology of extracellular vesicles. Nat Rev Mol Cell Biol. 2018; 19: 213-28.
19. Li Y, Yang YY, Ren JL, Xu F, Chen FM, Li A. Exosomes secreted by stem cells from human exfoliated deciduous teeth contribute to functional recovery after traumatic brain injury by shifting microglia M1/M2 polarization in rats. Stem Cell Res Ther. 2017; 8: 198.
20. Li Z, Li Y, Jiao J. Neural progenitor cells mediated by H2A.Z.2 regulate microglial development via Cxcl14 in the embryonic brain. Proc Natl Acad Sci U S A. 2019; 116: 24122-32.
21. Li Y, Wang X, Ren J, Wu X, Li G, Fan Z, et al. Mandible exosomal ssc-mir-133b regulates tooth development in miniature swine via endogenous apoptosis. Bone Res. 2018; 6: 28.
22. Renneville A, Van Galen P, Canver MC, McConkey M, Krill-Burger JM, Dorfman DM, et al. EHMT1 and EHMT2 inhibition induces fetal hemoglobin expression. Blood. 2015; 126: 1930-9.

23. Cereijo R, Gavalda-Navarro A, Cairo M, Quesada-Lopez T, Villarroya J, Moron-Ros S, et al. CXCL14, a Brown Adipokine that Mediates Brown-Fat-to-Macrophage Communication in Thermogenic Adaptation. Cell Metab. 2018; 28: 750-63 e6.
24. Gazarian KG, Ramirez-Garcia LR. Human Deciduous Teeth Stem Cells (SHED) Display Neural Crest Signature Characters. PLoS One. 2017; 12: e0170321.
25. Zhu Y, Zhang P, Gu RL, Liu YS, Zhou YS. Origin and Clinical Applications of Neural Crest-Derived Dental Stem Cells. Chin J Dent Res. 2018; 21: 89-100.
26. Xiao C, Wang K, Xu Y, Hu H, Zhang N, Wang Y, et al. Transplanted Mesenchymal Stem Cells Reduce Autophagic Flux in Infarcted Hearts via the Exosomal Transfer of miR-125b. Circ Res. 2018; 123: 564-78.
27. Wang C, Zhu G, He W, Yin H, Lin F, Gou X, et al. BMSCs protect against renal ischemia-reperfusion injury by secreting exosomes loaded with miR-199a-5p that target BIP to inhibit endoplasmic reticulum stress at the very early reperfusion stages. FASEB J. 2019; 33: 5440-56.
28. Su T, Xiao Y, Xiao Y, Guo Q, Li C, Huang Y, et al. Bone Marrow Mesenchymal Stem Cells-Derived Exosomal MiR-29b-3p Regulates Aging-Associated Insulin Resistance. ACS Nano. 2019; 13: 2450-62.
29. Zhang MZ, Wang X, Wang Y, Niu A, Wang S, Zou C, et al. IL-4/IL-13-mediated polarization of renal macrophages/dendritic cells to an M2a phenotype is essential for recovery from acute kidney injury. Kidney Int. 2017; 91: 375-86.
30. Lu H, Wu L, Liu L, Ruan Q, Zhang X, Hong W, et al. Quercetin ameliorates kidney injury and fibrosis by modulating M1/M2 macrophage polarization. Biochem Pharmacol. 2018; 154: 203-12.
31. Hayakawa K, Wang X, Lo EH. CD200 increases alternatively activated macrophages through cAMP-response element binding protein - C/EBP-beta signaling. J Neurochem. 2016; 136: 900-6.
32. Lin Y, Zhao JL, Zheng QJ, Jiang X, Tian J, Liang SQ, et al. Notch Signaling Modulates Macrophage Polarization and Phagocytosis Through Direct Suppression of Signal Regulatory Protein alpha Expression. Front Immunol. 2018; 9: 1744.
33. Xiang B, Xiao C, Shen T, Li X. Anti-inflammatory effects of anisalcohol on lipopolysaccharide-stimulated BV2 microglia via selective modulation of microglia polarization and down-regulation of NF-kappaB p65 and JNK activation. Mol Immunol. 2018; 95: 39-46.
34. Zhang RH, Judson RN, Liu DY, Kast J, Rossi FM. The lysine methyltransferase Ehmt2/G9a is dispensable for skeletal muscle development and regeneration. Skelet Muscle. 2016; 6: 22.
35. Eissenberg JC, Elgin SC. HP1a: a structural chromosomal protein regulating transcription. Trends Genet. 2014; 30: 103-10.
36. Huising MO, van der Meulen T, Flik G, Verburg-van Kemenade BM. Three novel carp CXC chemokines are expressed early in ontogeny and at nonimmune sites. Eur J Biochem. 2004; 271: 4094-106.
37. Rostene W, Guyon A, Kular L, Godefroy D, Barbieri F, Bajetto A, et al. Chemokines and chemokine receptors: new actors in neuroendocrine regulations. Front Neuroendocrinol. 2011; 32: 10-24.

38. Abarbanell AM, Coffey AC, Fehrenbacher JW, Beckman DJ, Herrmann JL, Weil B, et al. Proinflammatory cytokine effects on mesenchymal stem cell therapy for the ischemic heart. Ann Thorac Surg. 2009; 88: 1036-43.
39. Holan V, Hermankova B, Krulova M, Zajicova A. Cytokine interplay among the diseased retina, inflammatory cells and mesenchymal stem cells - a clue to stem cell-based therapy. World J Stem Cells. 2019; 11: 957-67.
40. Remberger M, Sundberg B. Cytokine production during myeloablative and reduced intensity therapy before allogeneic stem cell transplantation. Haematologica. 2004; 89: 710-6.

Figures

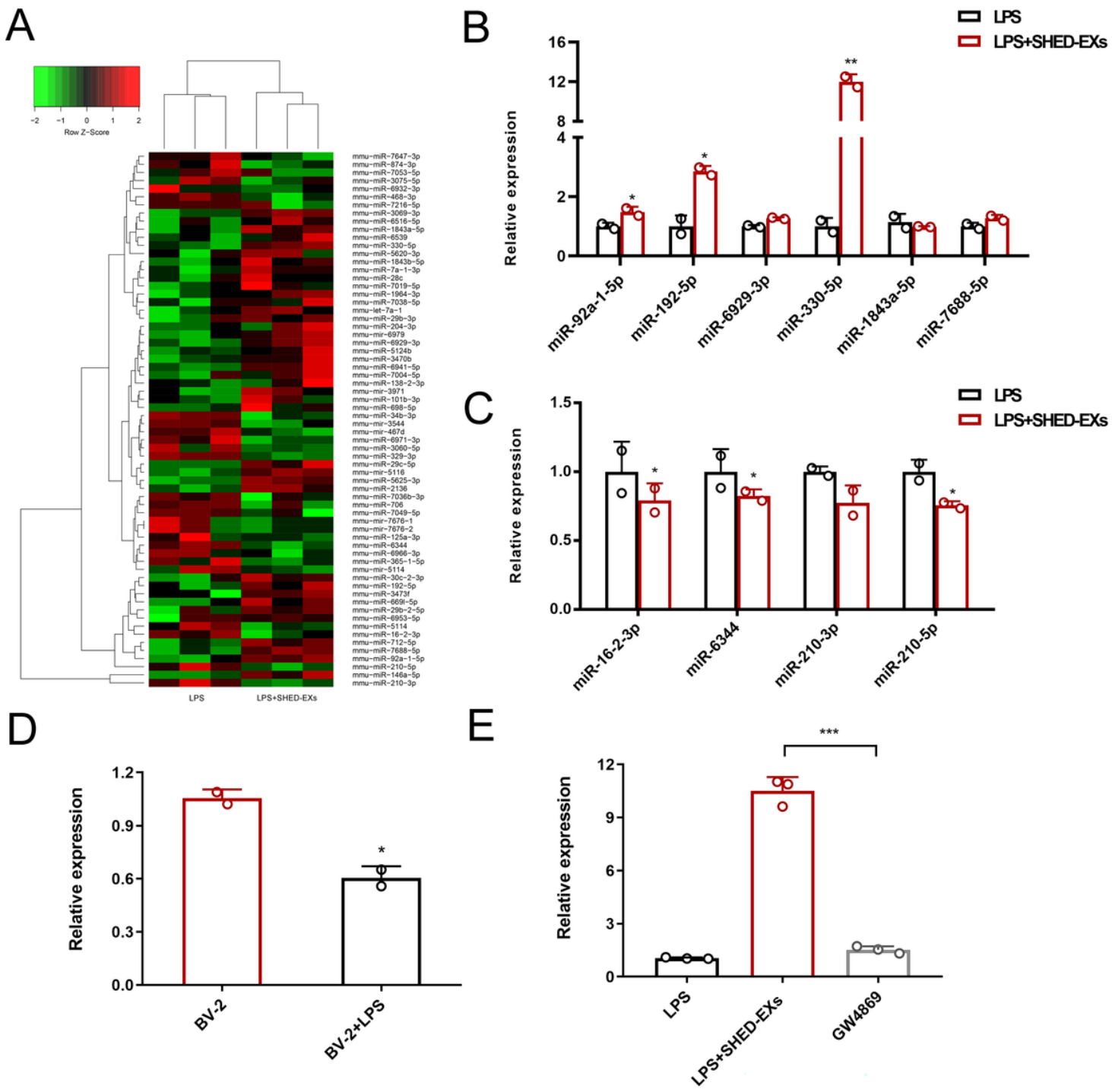

Figure 1

Differentially expressed miRNAs in microglia after SHED-EXs treatment. (A) miRNA microarray analysis of BV-2 after co-culture with SHED-EXs. (B) Real-time PCR validation of candidate miRNAs. *p < 0.05; **p < 0.01. (C) miR-330-5p expression in BV-2 after LPS stimulation. *p < 0.05. (D) Inhibition of EXs with GW4869 blocked delivery of exosomal miR-330-5p to BV-2. ***p < 0.001.

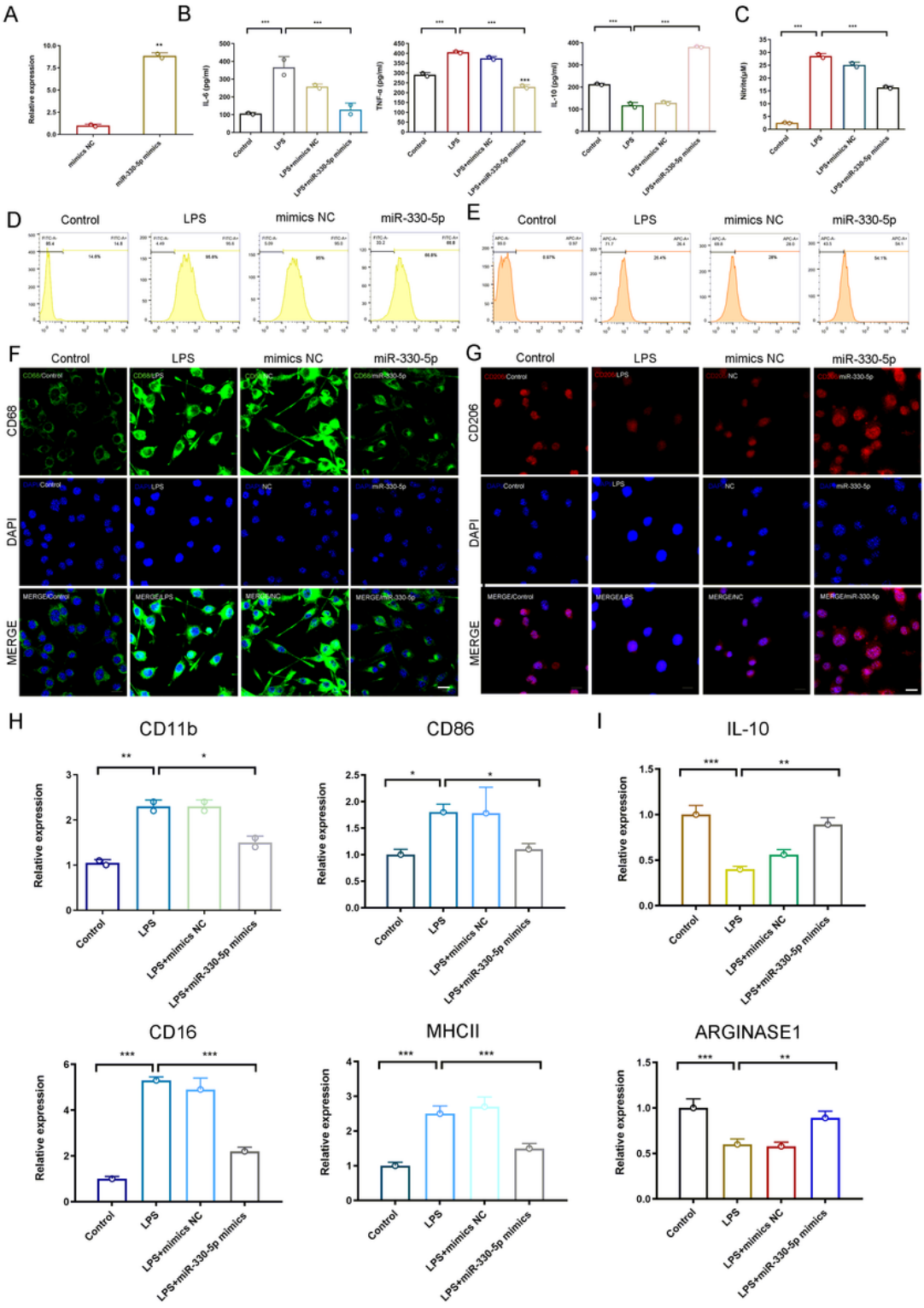

Figure 2

miR-330-5p inhibits microglial M1 polarization and promotes M2 polarization. (A) Transfection efficiency of miR-330-5p mimics. **p < 0.01. (B) IL-6, TNF-α and IL-10 levels in BV-2 supernatant quantified via ELISA. ***p < 0.001. (C) NO levels quantified via Griess assay. ***p < 0.001. (D) Representative flow cytometry plots of CD68 expression. (E) Representative flow cytometry plots of CD206 expression. (F) Representative image of immunofluorescent staining for CD68 (green), DAPI (blue). Scale bar: 50 μm. (G)

Representative image of immunofluorescent staining for CD206 (red), DAPI (blue). Scale bar: 50 μm. (H) Real-time PCR for the expression of microglial M1 polarization markers. *p < 0.05; **p < 0.01; ***p < 0.001. (I) Real-time PCR for the expression of microglial M2 polarization markers. **p < 0.01; ***p < 0.001.

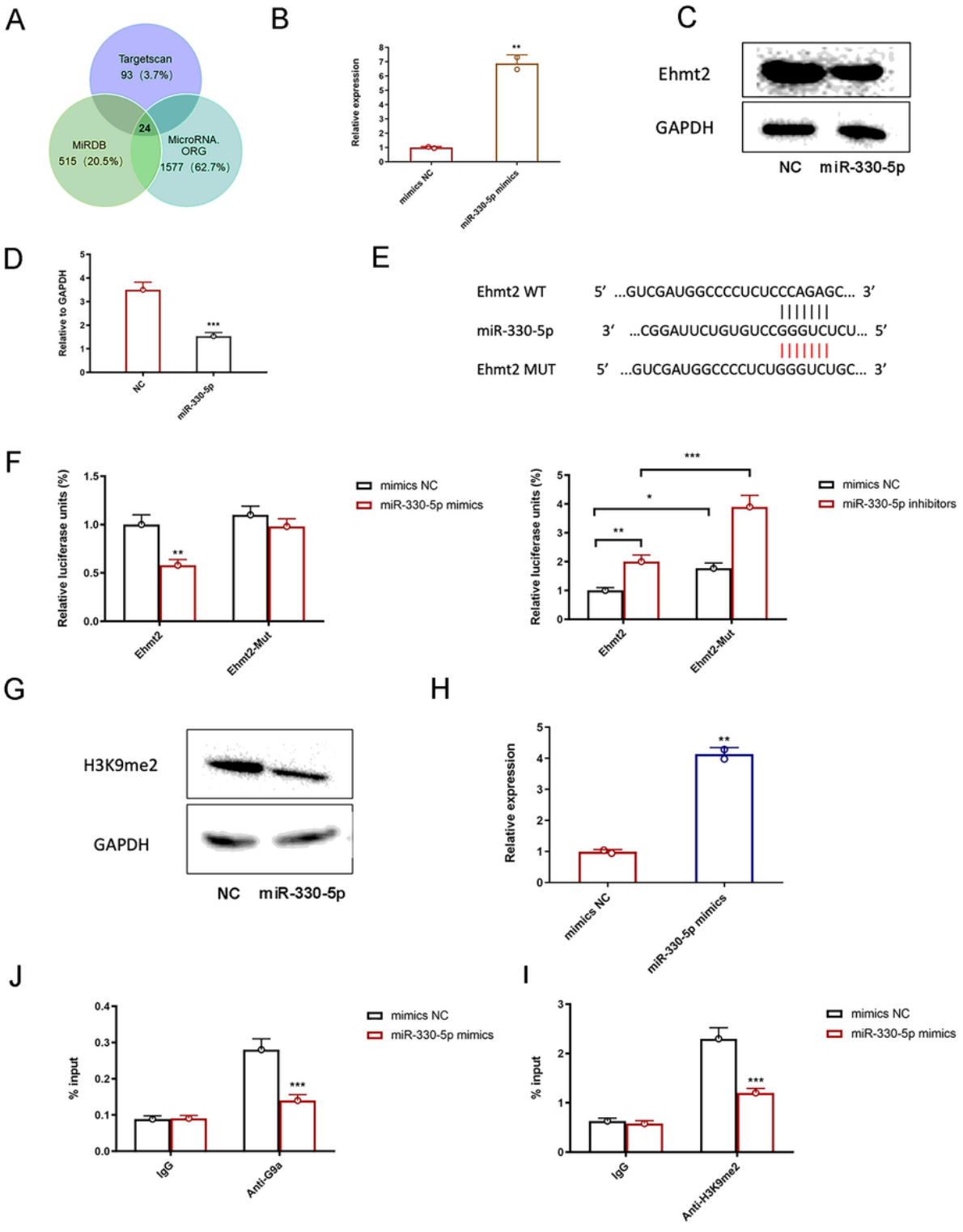

Figure 3

miR-330-5p targets Ehmt2 to promote CXCL14 transcription through H3K9me2 in the regulation of microglial polarization. (A) Overlapping data of predicted target genes of miR-330-5p from three

databases. (B) The expression of Ehmt2 in miR-330-5p overexpressed BV-2. **p < 0.01. (C) Protein level of Ehmt2 detected by Western blotting. GAPDH was used as control. (D) Quantitative analysis of Western Blotting. ***p < 0.001. (E) Luciferase reporter containing the 3' UTR of Ehmt2 with either wild-type (WT) or mutant (MUT) miR-330-5p target site. (F) Luciferase reporter assay to determine the relationship between miR-330-5p and Ehmt2. *p < 0.05; **p < 0.01; ***p < 0.001. (G) Protein level of H3K9me2 detected by Western blotting. GAPDH was used as control. (H) Expression of CXCL14 in miR-330-5p-overexpressing BV-2. **p < 0.01. (I) miR-330-5p overexpression decreased Ehmt2 levels at the promotor of CXCL14. **p < 0.01. (J) miR-330-5p overexpression decreased H3K9me2 levels at the promotor of CXCL14. ***p < 0.001.

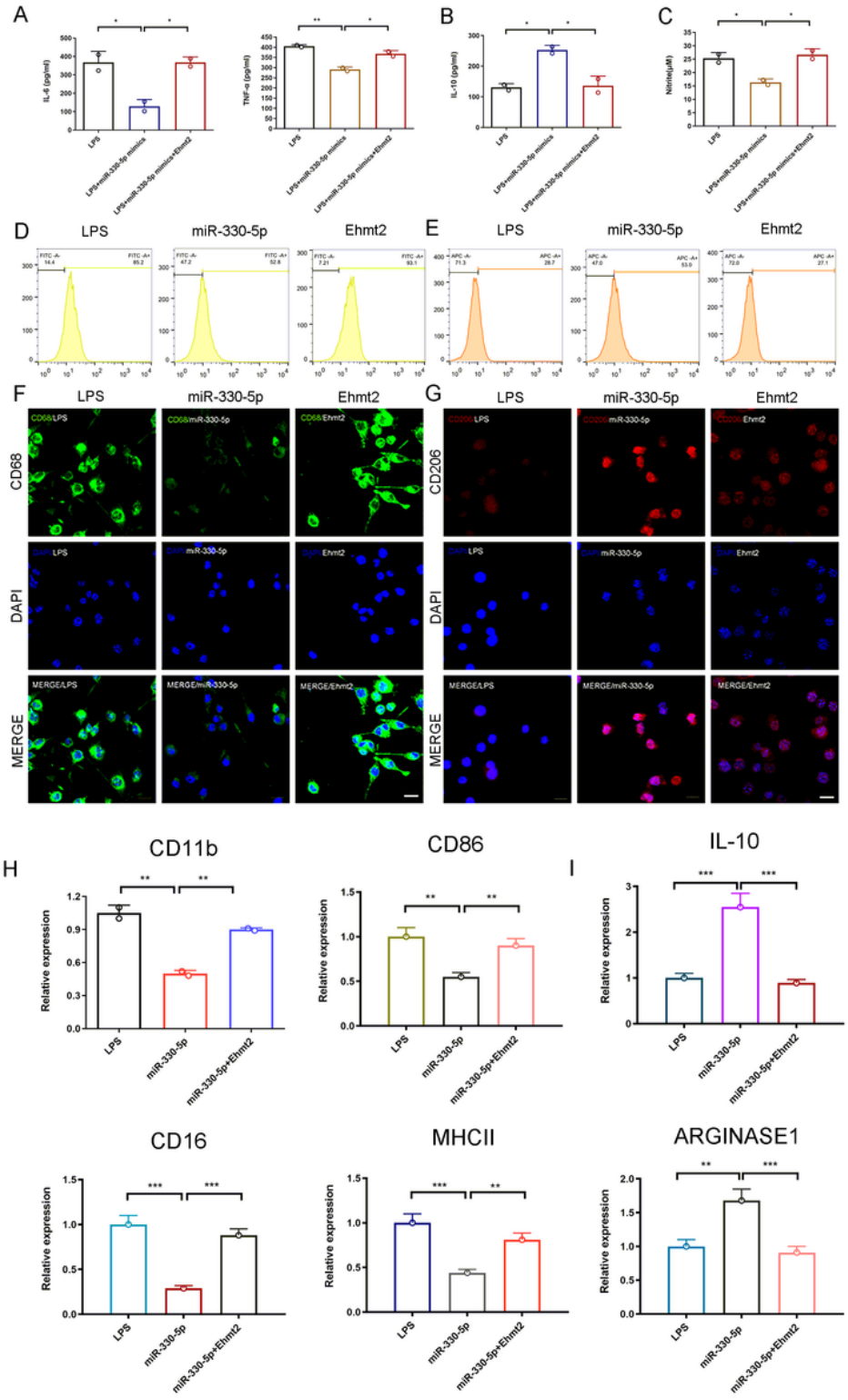

Figure 4

Ehmt2 rescues the inhibition of M1 polarization and promotion of M2 polarization of microglia mediated by miR-330-5p. (A) IL-6 and TNF-α levels in BV-2 supernatant quantified via ELISA. *p < 0.05; **p < 0.01. (B) IL-10 levels in BV-2 supernatant. *p < 0.05. (C) NO levels quantified via Griess assay. *p < 0.05. (D) Representative flow cytometry plots of CD68 expression. (E) Representative flow cytometry plots of CD206 expression. (F) Representative image of immunofluorescent staining for CD68 (green), DAPI

(blue). Scale bar: 50 μm. (G) Representative image of immunofluorescent staining for CD206 (red), DAPI (blue). Scale bar: 50 μm. (H) Real-time PCR for the expression of microglial M1 polarization markers. **p < 0.01; ***p < 0.001. (I) Real-time PCR for the expression of microglial M2 polarization markers. **p < 0.01; ***p < 0.001.

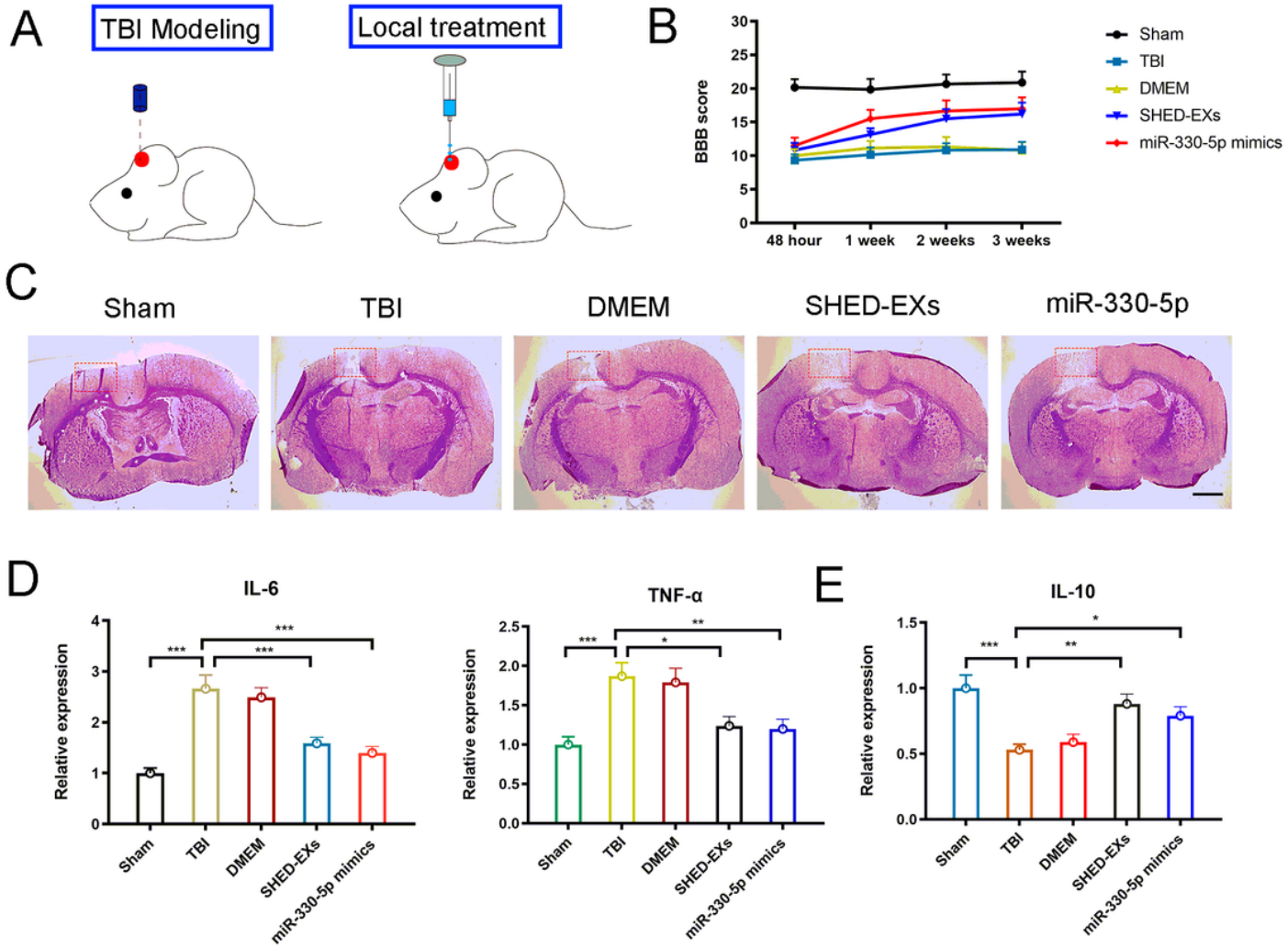

Figure 5

miR-330-5p ameliorates traumatic brain injury in rats. (A) TBI modeling and SHED-EXs/miR-330-5p treatment. (B) BBB scores of motor function. (C) Hematoxylin and eosin staining of damaged brain tissue. Scale bar: 200 μm. (D) Expression of IL-6 and TNF-α in brain tissues at 48 h after SHED-EXs/miR-330-5p treatment. *p < 0.05; **p < 0.01; ***p < 0.001. (E) Expression of IL-10 in brain tissues at 48 h after SHED-EXs/ miR-330-5p treatment. *p < 0.05; **p < 0.01; ***p < 0.001.

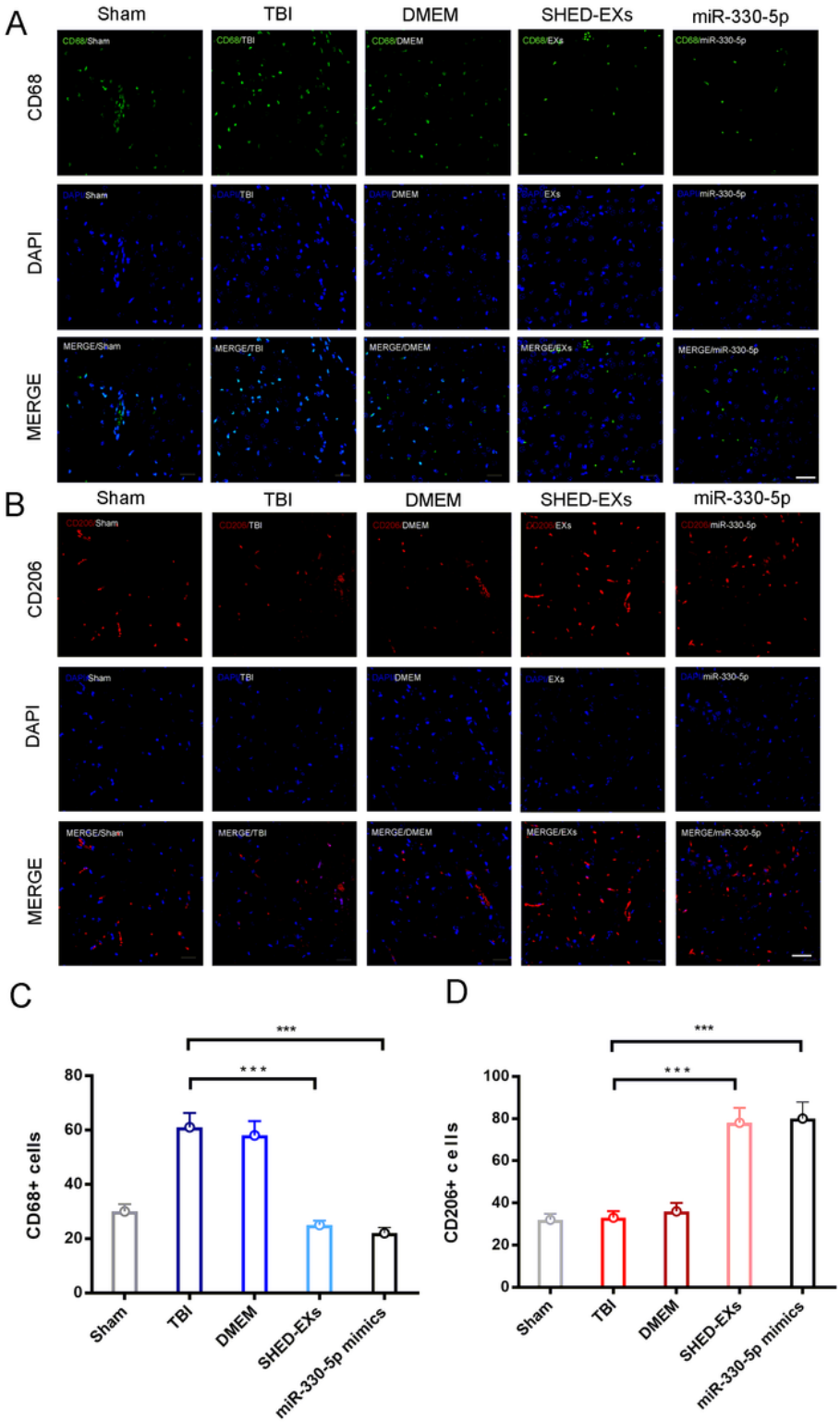

Figure 6

miR-330-5p inhibits microglial M1 polarization and promotes M2 polarization to ameliorate neuro-inflammation. (A) Representative image of immunofluorescent staining for CD68 in brain tissues at 48 h after SHED-EXs/miR-330-5p treatment. Scale bar: 100 μm. (B) Representative image of immunofluorescent staining for CD206 in brain tissue at 48 h after SHED-EXs/miR-330-5p treatment.

Scale bar: 100 μm. (C) Quantitative analysis of CD68 immunofluorescence. ***p < 0.001. (D) Quantitative analysis of CD206 immunofluorescence. ***p < 0.001.

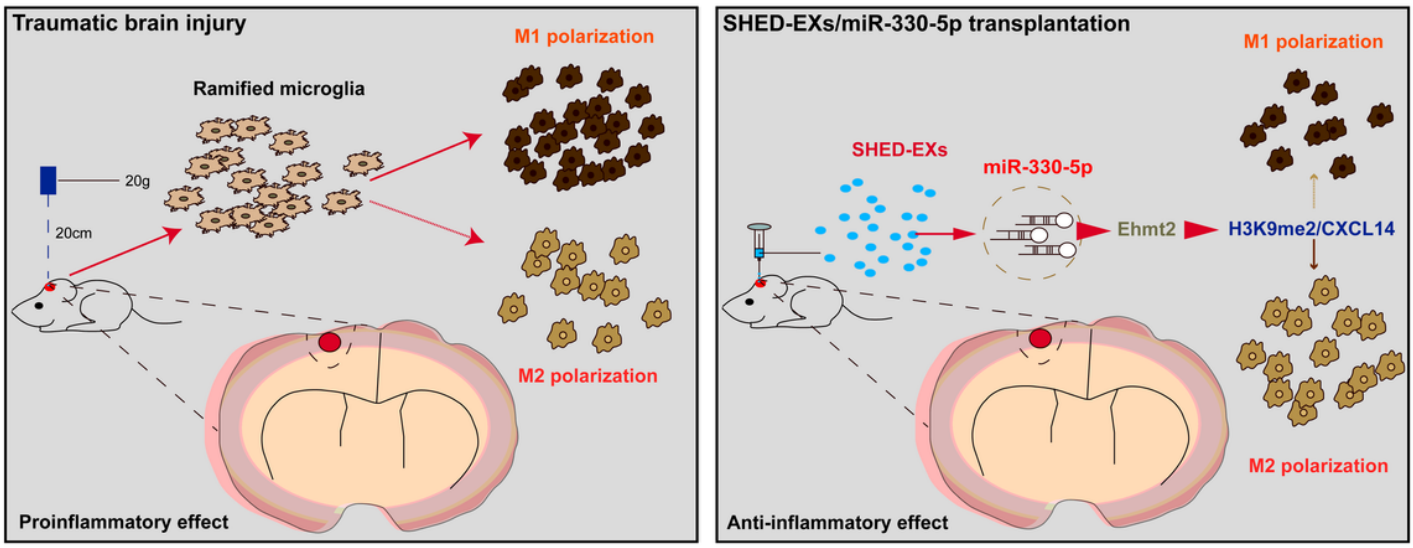

Figure 7

Schematic diagram of TBI pathology and the mechanism of SHED-EXs/miR-330-5p treatment. miR-330-5p from SHED-EXs ameliorates functional impairment caused by TBI by promoting M2 polarization and inhibiting M1 polarization to reduce neuro-inflammation and promote tissue repair through the Ehmt2-H3K9me2-CXCL14 axis.

Supplementary Files

This is a list of supplementary files associated with this preprint. Click to download.

- Appendixfile1.docx